Quantification of Specimen Geometry Effects on the Master Curve and T_o Reference Temperature

J.A. Joyce[1] and R.L. Tregoning[2]

[1]Department of Mechanical Engineering, US Naval Academy, Annapolis, MD USA
[2]Naval Surface Warfare Center, Carderock, MD USA

ABSTRACT

Application of the Master Curve method and associated reference temperature of ASTM E1921 to define the ductile to brittle transition in ferritic structural steels used in commercial nuclear reactor vessels requires extensive experimental verification. Recent suggestions have proposed replacing the nil-ductility reference temperature RT_{NDT} of the ASME Boiler and Pressure Vessel Code with a RT_{To} reference temperature. This reference temperature could then be used to position the median and lower bound transition toughness curves for the purpose of thermal shock evaluations or for life extension of existing US commercial nuclear power stations. In this experimental program different C(T), SE(B), and pre-cracked Charpy specimen geometries have been investigated including both deep and shallow cracked SE(B) geometries. Two or more test temperatures were used for each geometry and at least 6 identical specimens of each specimen configuration have been tested at each temperature. Specimen geometries have ranged from 5 mm thick SE(B) specimens to standard 1T (25mm by 50 mm) three point bend specimens and crack length to specimen width ratios for the SE(B) specimens ranged from a/W = 0.12 to 0.6. The material utilized was an A533 Grade B steel obtained from the decommissioned Shoreham nuclear power plant pressure vessel. Three distinct populations of data appear to exist in the results of this program corresponding to C(T) specimens, SE(B) specimens, and shallow crack SE(B) specimens. The differences found between shallow and deep crack specimens is not surprising, but the magnitude of the differences found between the C(T) and deep crack SE(B) specimens was highly unexpected and does not appear to have been previously reported.

INTRODUCTION

Earlier work [1] demonstrated that T_o estimates from precracked Charpy specimens are systematically 5 to 10^{o}C below estimates from C(T) specimens. This difference was found for a variety of materials and by several different investigators. While [1] postulated that this difference could be attributed to constraint loss in the Charpy geometry at large deformation, the Charpy bias remained evident in data-sets with little plastic deformation. Additionally, the T_o difference between Charpy and "large" SE(B) specimens (both rectangular and square cross-section greater than 1T thickness) was not as significant. These observations led to a comprehensive testing program using a single material to evaluate differences among various common specimen geometries. The test material is a 150 mm thick, A533B plate obtained from the Shoreham boiling water reactor. The reactor was fabricated, but only put into service for a short time.

The C(T), SE(B), and square-cross section bend bar geometries were studied. Specimen size and thickness was varied from 1T down to 0.2T and two to three thickness combinations were evaluated for

each unique specimen type. The 1T C(T) specimen geometry was initially tested at four temperatures above and below the estimated T_o to provide an accurate baseline T_o measurement. The other geometries were then tested at or near several of the 1T C(T) specimen test temperatures to develop separate T_o estimates. The test temperatures used for the smaller geometries were chosen to comply with the ASTM E1921 requirements in order to minimize constraint loss. Additional testing was conducted using short crack ($a/W < 0.15$) bend specimens in order to quantify the effect of significant crack-tip constraint loss on T_o. The 1T SE(B), 1/2T SE(B) and 1x1 square-cross section geometries were studied, and the test temperatures were similar to the standardized, deep crack testing.

EXPERIMENTAL DETAILS

The A533B test material was extracted from a portion of the 150 mm thick shell plate from the decommissioned Shoreham nuclear plant boiling water reactor pressure vessel. The test piece was originally located in the upper section of the vessel just below the nozzle inserts. The tensile-mechanical properties at four temperatures are presented in Table 1. Results presented in [1] illustrate that this plate material has uniform tensile properties throughout the central 100 mm of the plate. All specimens were machined from a block that measured 30 cm along the rolling direction by 214 cm in the transverse direction. The Table 1 properties represent the averages of specimens taken throughout this central region of the plate.

TABLE 1
A533B TENSILE MECHANICAL PROPERTIES

Temp. (^oC)	σ_{Ys} (MPa)	σ_{ult} (MPa)	% Elong. (25 mm)	% R.A.
-120	603	760	28	63
-80	569	733	32	67
24	488	644	28	70
115	445	589	23	70

The test matrix containing the specimen geometries evaluated and the chosen test temperatures is summarized in Table 2. This table summarizes the parameters for the current database of 168 standard fracture toughness values for this material. Of these results, 153 results are uncensored as per ASTM E1921 requirements. The test matrix is comprehensive in that all the typical test geometries were evaluated at more than one test temperature with respect to the best estimate T_o. The following is a brief description of the specimen preparation and testing details. Further information on this test plan is available in reference [2].

In Table 2, the specimen size description follows the standard ASTM E399 convention of xT, where x is the nominal specimen thickness, B_{max}. Three distinct specimen geometries were studied: a square cross-section single-edged notch bend geometry, a standard rectangular cross-section single-edged notch bend {SE(B)} geometry, and the compact tension {C(T)} geometry. The planar dimensions for each specimen type scale self-similarly with respect to B_{max} so that the specimen width (W) to B_{max} ratio is constant for each geometry regardless of absolute specimen size. The $W/B = 2$ for the C(T) and SE(B) specimens, while $W/B = 1$ for the square cross section bend geometries. Additionally, several SE(B) and square bend specimens were tested with $a/W < 0.15$. A total of 35 tests were conducted for these low constraint geometries. The T_{oq} values representative of these geometries obviously are not expected to be equivalent to the "material" T_o and are not valid tests within the context of E1921.

The majority of the specimens were side-grooved after pre-cracking with a 0.25mm radius and a depth corresponding to the total thickness reduction indicated in Table 2. All specimens were oriented with the crack in the L-S direction as defined by ASTM E399. An effort was made to conduct testing at similar temperatures for each geometry type so that 1T corrected values could be compared directly.

TABLE 2
MATRIX OF TEST DATA FOR A533B STEEL

Specimen Geometry	Size (B_{max})	a/W	SG Depth (%of B_{max})	Test Temp. (^oC)	N	M_{KJcmed}	T_o or T_{oq} ^oC
Deep Crack Testing							
SE(B)	1T	0.5	0	-118	10	536	-95.9
	1/2T	0.52	20	-116	8	295	-87.7
		0.52	20	-79	8	76	-101.3
	0.2T	0.56	20	-130	9	152	-85.4
		0.48	20	-114	8	107	-92.6
Square Bend	1T	0.51	10	-118	8	272	-94.5
		0.51	10	-76	8	87	-94.2
	0.394T	0.5	20	-115	8	157	-73.6
		0.5	20	-83	16	59	-83.8
C(T)	1T	0.55	20	-40	14	94	-74.2
		0.50	20	-85	8	351	-78.7
		0.50	20	-110	8	818	-67.5
0.8T Plan C(T)	1T	0.50	20	-60	7	117	-84.0
		0.50	20	-80	7	273	-74.6
C(T)	1/2T	0.55	20	-39	13	33	-84.3
		0.57	20	-86	8	146	-81.2
		0.55	20	-118	6	310	-84.6
Short Crack Testing							
SE(B)	1T	0.15	0	-120	5	930	-97.1
	1/2T	0.12	20	-115	6	214	-123.7
		0.12	20	-96	8	188	-108.5
Square Bend	1T	0.12	10	-120	8	97	-126.6
		0.12	10	-92	8	352	-110.0

The other specimen types were tested largely at –80^{o}C, and between –110 to –120^{o}C. For the smallest specimen types, testing was necessary below –120^{o}C to ensure that the E1921 deformation criteria could be met. A few of the short crack specimen data sets were evaluated near –95^{o}C to generate significant constraint loss while avoiding ductile tearing during the tests. Temperature control was achieved by using a convection chamber with a liquid nitrogen spray used to cool the specimens. Temperatures were constant within ±2^{o}C for an individual test, and replicate temperature control for all specimens comprising a data set was within ±3^{o}C. All specimen pre-cracking and testing requirements adhered to ASTM E1921 as appropriate. Tests were conducted at quasi-static test rates (≈ 0.5 – 1.0 MPa$\sqrt{m}$/s) in a servo-hydraulic test machine.

PRESENTATION OF RESULTS

The T_o results obtained from the data sets described above are summarized in Table 2. The 1T size corrected K_{Jc} results obtained from C(T) specimens are plotted in Figure 1 as a function of test temperature. Results which are censored as per ASTM E1921 are indicated in the figure. The C(T) data is an amalgam of the 1T, 1/2T and 25.4mm, 0.8T plan C(T) results. This data-set yields a best estimate T_o value of -78 ^{o}C and the data appears to fit well between about the median curve and within the confidence bounds. The T_o value for individual data-sets are also very consistent and fall within ±10 ^{o}C of the multi-temperature value (Table 2). Figure 2 shows results obtained from the square cross section bend and SE(B) specimens. The best estimate T_o value was found to be –90^{o}C for this grouping, a considerably different value than the -78^{o}C result obtained for the C(T) specimens. Figure 2 also shows the Master curve and confidence bounds for the C(T) specimens and it is clear that a considerable difference exists between the SE(B) and C(T) data sets. The thickness ranged from 0.2T to 1T for these specimens as indicated in Table 2. It is interesting to note that the individual T_o values for data-sets with the SE(B) type geometry fell between -85^{o}C and –97^{o}C. The square bend specimens also resulted in T_o values within this range (-94^{o}C), but the Charpy T_o values were lower than any of the other estimates (T_o = -74^{o}C and –81^{o}C) for this specimen type. Figure 3 compares the C(T) specimen master curve and

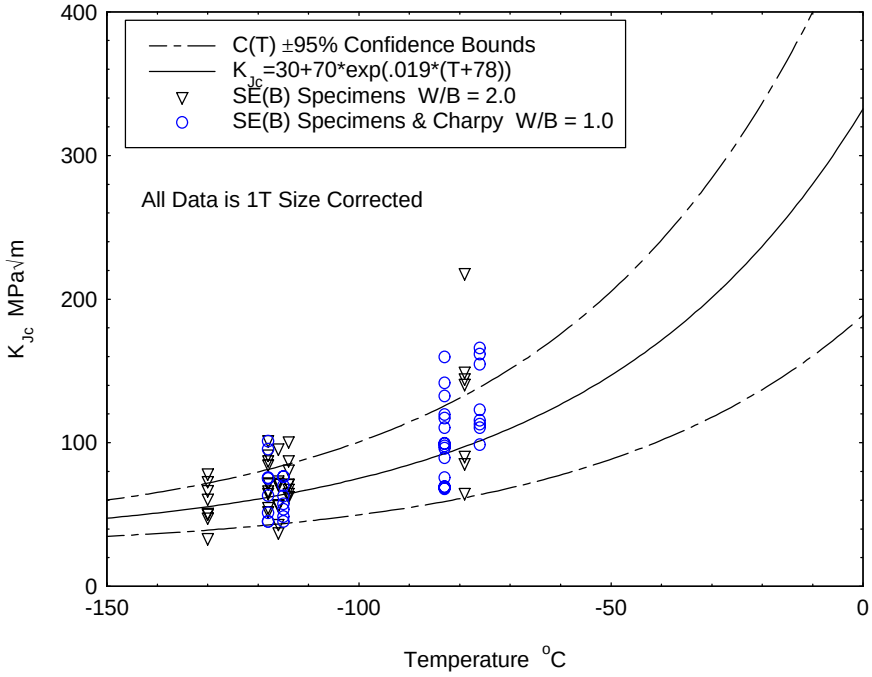

Figure 1: Baseline C(T) data set used to evaluate T_o and the ASTM E1921 Master curve for the Shoreham vessel material.

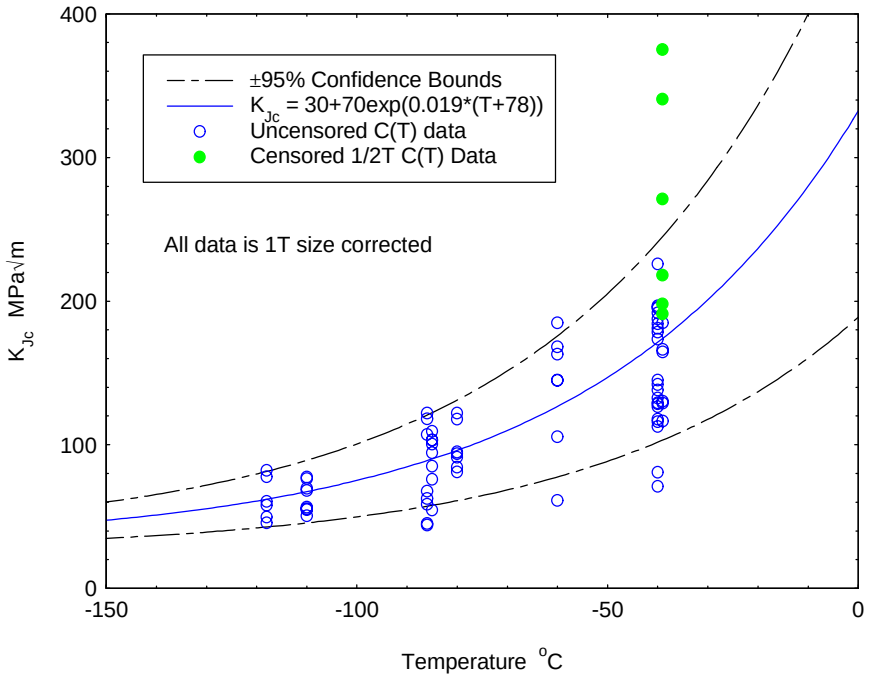

Figure 2: Comparison of SE(B), square bend, and Charpy specimen results with the Master curve and confidence bounds from the C(T) specimens.

confidence bounds with the deep and shallow crack square bend and SE(B) data. This plot (and T_o values in Table 2) illustrates that the toughness measured in the shallow crack bend bar geometries is elevated compared with both the C(T)-based results and the results of standard deep crack SE(B) specimens.

Three distinct populations of data appear to exist in this data set corresponding to C(T) specimens, SE(B) specimens, and shallow crack SE(B) specimens. No distinct separation was found for the square bend geometry in comparison with the standard deep crack SE(B) geometry. This result implies that specimen geometry influences transitional cleavage fracture in this material. The question exists if this is a real phenomenon, or is due to statistical uncertainty or simply results from material variability.

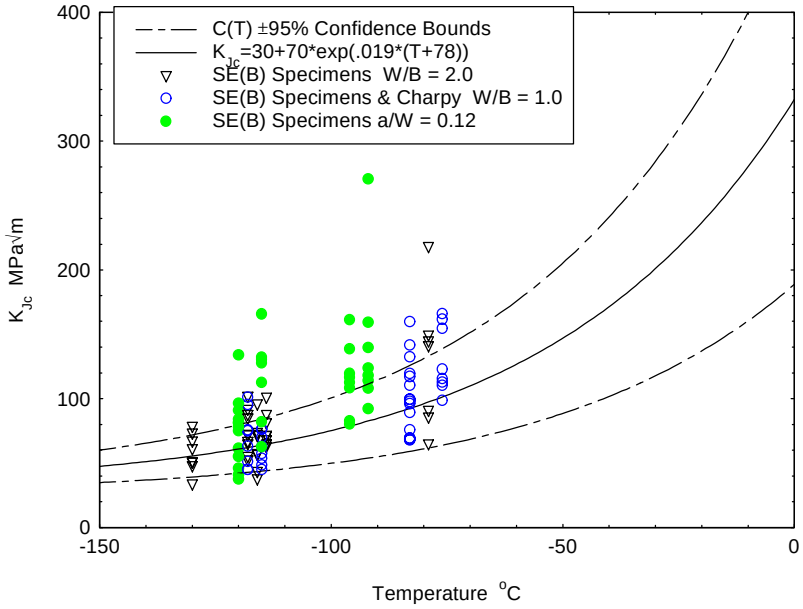

Figure 3: Comparison of shallow crack SE(B) results with square bend and SE(B) data and with the Master curve and confidence bounds from the C(T) data sets.

It is helpful to compare the results as a function of specimen type to answer this question. The combined best estimate value of T_o (T_{obe}) for this material using all available, valid results was first calculated to be –85°C (168 specimens). Individual values of T_o were determined for each unique specimen geometry using the multi-temperature procedure proposed by Wallin[3]. A unique geometry is defined for each distinct specimen thickness and plan cross-section type. The individual T_o values utilized all ASTM E1921 valid data for a unique geometry and values represent data taken at multiple temperatures as defined in Table 2. Figure 4 illustrates the differences in T_o as a function of specimen geometry with respect to T_{obe}. The 95% confidence limits have been included to estimate the uncertainty due to sample size in the individual T_o values. These limits have been derived by weighting them with the appropriate scale parameter (β in E1921) for the 1T K_{Jcmed} value of each data set.

It is clear in Figure 4 that the C(T) (1T, 0.8T-plan, 1/2T) T_o estimates are always lower than T_{obe}, while the SE(B) (1T, 1/2T, 0.2T) T_o estimates are consistently higher. The 25 mm. square Bend results are mixed. The 25 mm square bend result is close to the SE(B) T_o grouping while the Charpy result falls closer to the C(T) data. However, the confidence limits due to sampling uncertainty do result in some overlap between the SE(B) and C(T) individual results. Other potential factors that could lead to the measured differences between specimen types include material variability and the deformation level (M) at fracture. Material variability was addressed initially by requiring all specimens to be tested within the central part of the plate, between the ¼T and ¾T locations. While there was no effort to ensure that the crack tips ended at the same absolute plate depth, several different depths were sampled for each specimen plan type (C(T), SE(B), Square bend).

Also, the specimen plan types were spread throughout the plate width so that they were not grouped within a single region of the plate. The deformation level also potentially influences the measured T_o value. As constraint decreases, the measured toughness at fracture increases and leads to a decrease in T_o. Specimen constraint can be quantified by the expression $M = Eb\sigma_{ys}/K_{Jc}^2$, where b is the remaining specimen ligament, σ_{ys} is the material yield strength, J_C is the value of the J-integral at cleavage (defined as K_{Jc}^2/E), and M is defined as the "constraint limit". As M decreases, the crack tip constraint at cleavage also decreases. ASTM E1921 requires data censoring for $M < 30$ in an effort to ensure that the K_{Jcmed} value of the data set is not affected by constraint loss. For this data set, the bulk of the testing was conducted at high M values as shown by the tabulated M values in Table 2. Only two data sets had $M_{KJcmed} < 70$. This implies that constraint loss during testing is not a reason for the differences in the measured T_o values for different specimen geometries found in this data set.

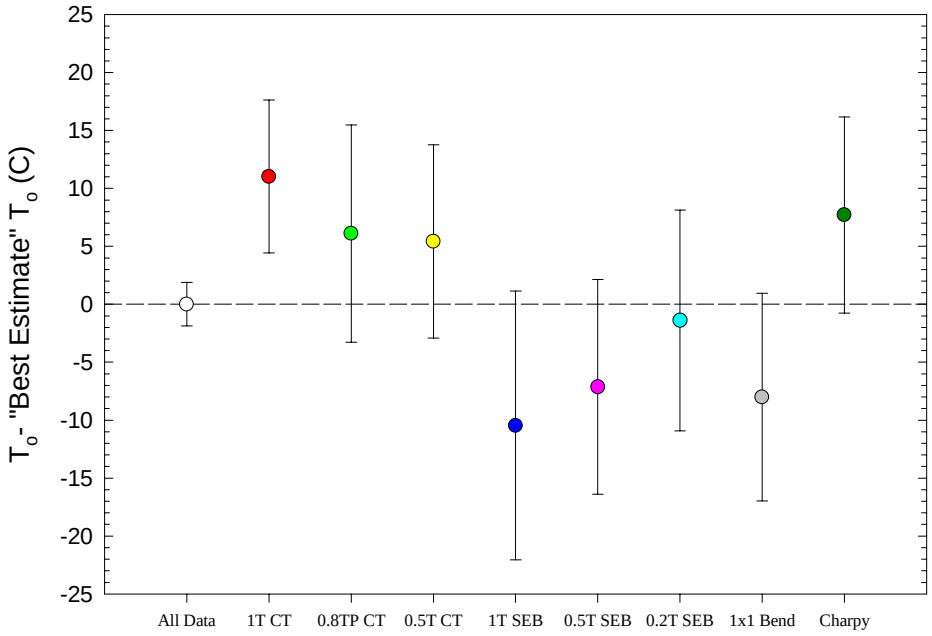

Figure 4 The combined best estimate T_o shown for each specimen geometry.

DISCUSSION

The T_o differences among different specimen geometries as a function of crack length implies that the stress field which triggers cleavage is not constant. Other research has noted differences in the magnitude and shape of the stress field as a function of geometry and loading mode [5]. This has been utilized to quantify toughness differences among different geometries in the past [6-7]. While this prior work has been largely successful it has concentrated on ductile upper shelf fracture behavior rather than differences in cleavage toughness between "low" and "high" constraint geometries.

The character of the linear elastic crack tip stress field at cleavage can be more completely described by the first two components (K, and T) in the asymptotic expansion of the crack tip stress field, σ_{ij} [8]:

$$\sigma_{ij} \rightarrow \frac{K}{\sqrt{2\pi r}} f_{ij}(\theta) + T\delta_{1i}\delta_{1j} \qquad (1)$$

In Eq. 1, $f_{ij}(\theta)$ is the angular variation of the crack-tip stress fields, r is the radial distance from the crack tip, K is the stress intensity factor, and T is defined as the T-stress. The T-stress is conceptually a non-singular stress component applied parallel to the crack tip. Negative T-stress values denote constraint loss with respect to SSY. The T-stress is proportional to the applied remote load (expressed through K_I) which motivates the following relationship:

$$T = \frac{BK_I}{\sqrt{\pi a}} \qquad (2)$$

Here, a is the crack depth and B is the "geometry ratio". The geometry ratio is independent of loading magnitude and is only a function of loading mode, specimen geometry, and crack length. It is therefore a convenient measure of constraint differences among particular geometries. The B parameters are determined for each in-plane geometry using the polynomial expressions presented in [10] corresponding to analyses of [9]. The nominal crack length has been utilized in each case. The T-stress has been determined from B using Eq. 2 and has been based on the 1T K_{Jcmed} value for the data-set.

Figures 5 and 6 illustrate the measured T_o (or T_q) values as a function of B and T-stress respectively. There is a clear monotonic relationship exhibited. Lower (increased negative) B or T-stress values result

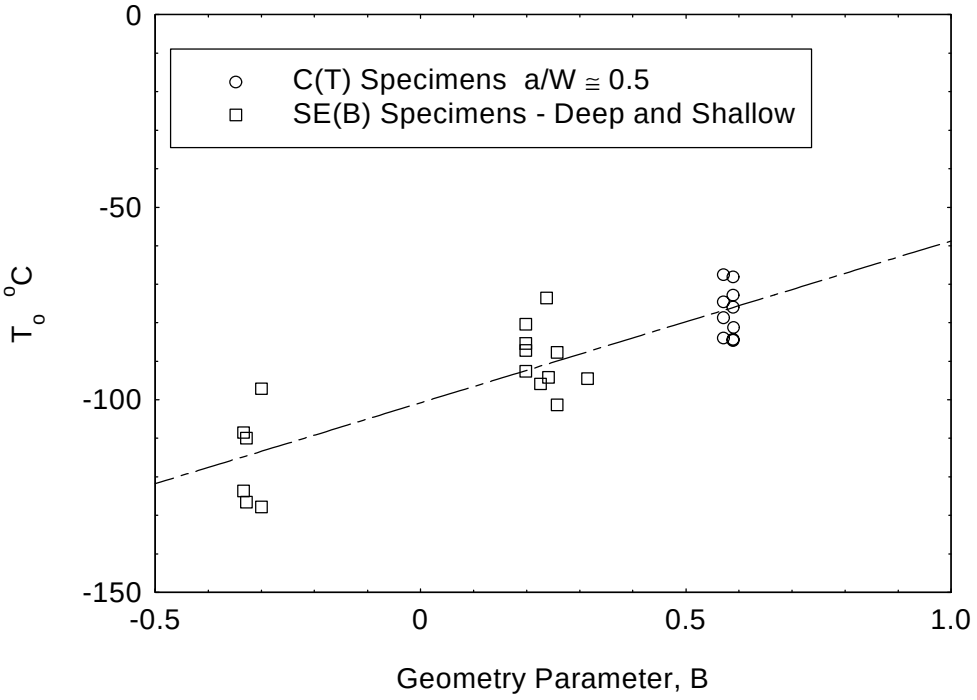

Figure 5: The reference temperature T_o shows a linear correlation with the T-Stress B geometry ratio.

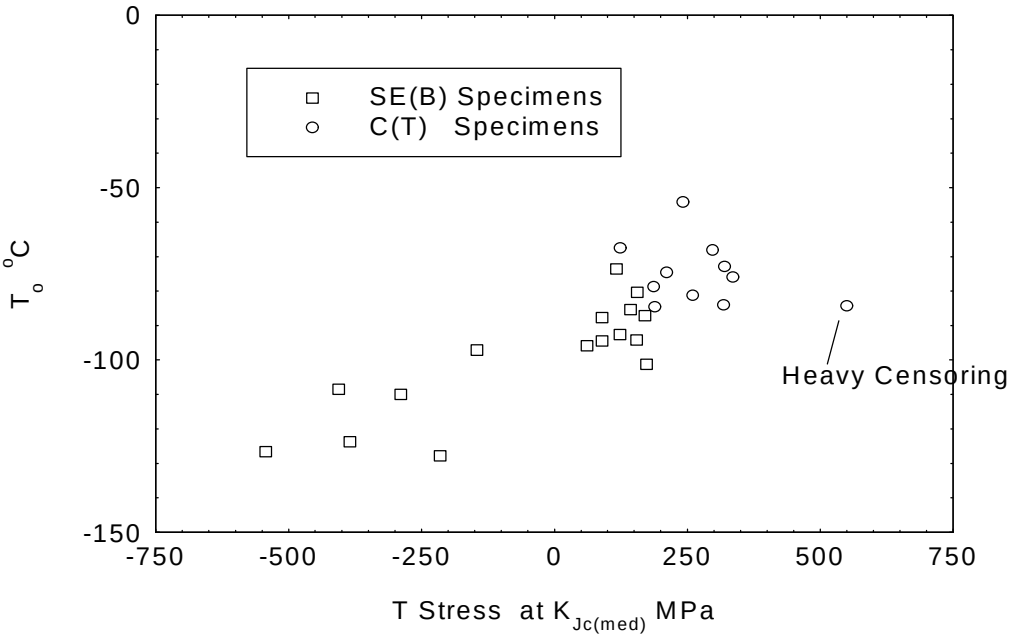

Figure 6: Dependence of the T_o reference temperature on the T-stress for all data sets.

in lower T_o (or T_q) measurements. Higher and even positive T-stress values result in higher T_o estimates. The direct comparison between T-stress and T_o can be somewhat misleading because both variables are monotonic functions of 1T K_{Jcmed}. The T-stress is linearly-dependent on 1T K_{Jcmed} while T_o exhibits a logarithmic dependence due to the master curve shape. Hence, a monotonic relationship between T_o and T-stress is largely preordained. However, the clear monotonic relationship between T_o and B is solely due to the effect of crack tip constraint on T_o since B is only a function of the specimen geometry and loading mode. This effect of constraint loss (measured by T-stress) has been previously used to describe toughness differences between deep crack and shallow crack SE(B) specimens. However, this is the first indication that the relationship appears to also extend to 0 and positive T-stress values. It has previously been argued that there should be little difference between measured toughness values in nominally "high constraint" deep crack geometries such as the C(T) and SE(B) specimens and these and other specimen types are currently allowed by fracture toughness standards like ASTM E399.

These results contradict this argument and show that B and toughness may be inexorably linked. The implication is that the existence of a constant "material toughness" is a fallacy. Cleavage toughness will always be a function of the material's properties and geometry as expressed through B. The fact that this relationship has not been previously documented is likely due to its subtlety. While the plastic zone shape and magnitude (expressed by B) differences among specimen types have been known for some time, there was no manifestation of this difference in measured results. Investigations on materials for which fracture was characterized by ductile hole growth fracture mechanisms, have demonstrated that specimen geometry and hence the T-stress has a minimal impact on J_{Ic} and the J-R curve up to prescribed deformation (or specimen capacity) limits[11]. Beyond these limits, constraint loss does affect the R-curve. However, for cleavage dominated fracture, the scatter in the results has precluded a rigorous evaluation of these differences. The master curve methodology specified in ASTM E1921 provides the framework necessary to uncover these differences. The size scaling criteria and toughness temperature relationship allows toughness differences as a function of specimen thickness and test temperature to be largely eliminated. Quantification of failure probability and confidence limits allows the toughness distributions to be evaluated using rigorous statistical tests.

CONCLUSIONS

The data illustrates statistically significant differences between the T_o values measured in C(T) (-78^{o}C) and bend specimens (-90^{o}C) for this A533B material. This measured difference does not appear to be related to absolute specimen size, as the results for different thickness specimens were generally consistent. This finding implies that cleavage toughness may explicitly be a function of specimen geometry and loading mode, which suggests that fracture standards like ASTM E399 should be revised when cleavage fracture occurs.

There is no statistically-significant measurable difference between T_o measured in square bend and SE(B) geometries. While the square bend results were closer to the SE(B) results, the pre-cracked Charpy T_o values were closer to the C(T) results. Shallow crack (a/W = 0.12 – 0.15) SE(B) specimens lead to lower T_o estimates due to toughness elevation compared to the deep crack specimens. The elevation is a function of test temperature and a/W ratio. This material exhibited as much as a 30^{o}C decrease in the specimen's T_q value compared to the deep crack SE(B) results.

The differences between the deep crack C(T), SE(B), and shallow crack SE(B) T_o (or T_q) values appear to be directly proportional to the non-dimensional T-stress (B) at the crack tip. Higher B values correspond to higher T_o (or T_q) values in this material.

REFERENCES

1. Joyce, J.A., Tregoning, R.L.(2000), to be published, *Engineering Fracture Mechanics*.
2. Tregoning, R.L., Joyce, J.A., submitted, *Engineering Fracture Mechanics*.
3. Wallin, K.(1995), In: *Constraint Effects in Fracture Theory and Applications: Second Volume*, ASTM, Conshohocken.
4. Larsson, S.G., Carlsson, A.J.(1973), *J. Mech. Phys. Solids* **21**, 447.
5. Betegon, C., and Hancock, J.W.(1991), *Journal of Applied Mechanics* **113**, 104.
6. Hancock, J.W.(1992), In: *Proceedings of the International Conference on Shallow Crack Fracture Mechanics Tests and Applications,"* TWI, Cambridge.
7. Sumpter, J.D.G.(1993), *Constraint Effects in Fracture*, ASTM , 492.
8. Williams, M.L.(1957), *J. Appl. Mech.* **24**, 109.
9. Kfouri, A.P.(1986), *Int. J. Fract.* **30**, 301.
10. Sherry, A.H., France, C.C., Goldthorpe, M.R.(1995), *Fatigue Fract. Engng Mater. Struct.* **18**, 141.
11. Joyce, J.A., Tregoning, R.L.(2000), In: *Fatigue and Fracture Mechanics: 30th Volume*, ASTM, Conshohocken, 357.